

## Preparation Of Ferrite Powders $BaFe_{(12-x)}Ti_xO_{19}$ , And Its Structural, Morphological & FTIR Study

Aparna.A.R.<sup>a</sup>, Brahmajirao.V<sup>b</sup>, & Kartikeyan.T.V.<sup>c</sup>

<sup>a</sup> Ph.D. Research Scholar, Department of Nanoscience and Technology, JNTU, Hyderabad, India

<sup>b</sup>(Previously) Matrix Institute of technology, Cheekatimamidi (V), Bommalaramaram (M), [Jawaharlal Nehru Technological University,] HYDERABAD, Pin Code – 508116, &

( at present)MGNIRSA, A Unit of D. Swami Nathan Research Foundation, Hyderabad-500029, A.P. INDIA

<sup>c</sup> Scientist 'F', ASL, DRDO, Hyderabad, India,

---

**Abstract:** This paper presents the preparation of Ti-doped barium ferrite powders  $BaFe_{(12-x)}Ti_xO_{19}$  for ( $x = 0.32$  and  $x=0.36$ ) nanomaterial using sol-gel route followed by the thermal insulation process and heat-treatment, recently reported by Wangchang Li et.al.,[1]. The pH of the medium and varying 'x' values were the aspects of concentration of our study in this communication. Nanomaterial is synthesized for the value of ( $x = 0.32$  and  $x=0.36$ ) at  $950^\circ C$  temperature. The phase structure and morphology were analysed by standard XRD, FTIR and SEM techniques.

**Keywords:** Barium ferrite, sol-gel route, Titanium, Nano ferrites, morphology.

---

### I. Introduction

Ferrites have attracted attention over the years as magnetic materials, because they are relatively inexpensive, stable and have a wide range of technological applications. The physical properties of ferrites are controlled by the preparation conditions, chemical composition, sintering temperature and time, type and amount of substitutions [2]. Ferrites exhibit outstanding microwave absorption properties and are widely employed in military and civil fields due to their high resistivity and severe EM energy attenuation, especially near the natural resonance frequency of magnetic moments [3-6].

In recent years, nano sized magnetic particles have drawn outstanding attention due to the unique mechanical, electrical, optical, and magnetic properties. Also nano sized magnetic particles have properties, which are drastically different from those of the corresponding bulk materials. Nanocrystalline barium ferrites are very interesting because of its chemical properties and thermal studies [7].

Due to the development of new technologies for radar and microwave communication, the research on microwave absorbing materials has increased in recent years. The main applications of these materials intend to reduce the human exposure to microwaves by means of absorbing coatings [8-10]. Ti-doped barium ferrite powder is an efficient absorber of electromagnetic waves in the microwave spectrum.

In the present communication the preparation & characterisation nanopowder of BFTO was prepared using sol-gel method. The prepared powders were characterized using X-ray Diffraction (XRD), Scanning Electron Microscopy (SEM) and Fourier Transform Infrared Spectroscopy (FTIR).

### Experimental procedure

The sol-gel combustion method has the unique advantage for the low costs using simple equipment in large-scale high-purity. Martirosyan et al. [11, 12] reported vivid contrasts in between Solution Combustion Synthesis (SCS) and carbon combustion synthesis of oxides (CCSO) in the synthesis of nano ferrites. The sol-gel combustion synthesis of hexagonal barium ferrite was reported to be especially conspicuous in the process of converting  $Fe_2O_3$  into barium ferrite.

M.J.Molaei et.al.,[13(a) and (b)],in his study on Magnetic property enhancement and characterization  $BaFe_{12}O_{19}/Fe_3O_4$  and  $Fe/Fe_3O_4$  magnetic nano-composites, reported the effects of milling time and heat treatment temperature on the characteristics of powder mixture. The powders were studied by X-ray diffraction analysis, vibrating sample magnetometry, transmission electron microscopy and Mossbauer spectroscopy. Phase analysis results showed that  $Fe_2O_3$  in barium ferrite partially reduced to  $Fe_3O_4$  during milling; hence, the reduced phase and remaining barium ferrite formed a nano-composite of  $BaFe_{12}O_{19}/Fe_3O_4$  after 20 h of milling  $Fe_3O_4$ . Heat treatment of the 40 h milled samples at  $750-900^\circ C$  resulted in formation of Fe containing nano-composite

The Flow chart and detailed procedure of the synthesis for the Ti-doped barium ferrite powders  $BaFe_{(12-x)}Ti_xO_{19}$  had been communicated in our earlier publication[17]

### Raw materials

The Synthesis of the chosen Nanomaterial for the study was done at National Chemical Laboratories, Pune, INDIA. Ti-doped barium ferrite powders were synthesized by the sol-gel method from the starting raw materials. Barium ferrite ( $BaFe_{12}O_{19}$ ) and Titanium(IV) butoxide( $Ti(OC_4H_9)_4$ ), [complete chemical formula being  $Ti(OCH_2CH_2CH_2CH_3)_4$ ] obtained from Sigma Aldrich. Citric acid, Ammonia, Absolute Ethyl alcohol and Deionized water were used as ancillary raw materials. These were procured from E-Merck and were eventually purified using prescribed standard chemical procedure.

### Synthesis of the samples

According to the composition of  $BaFe_{(12-x)}Ti_xO_{(19)}$  ( $x = 0.32$ ), three solutions were prepared. Solution (1) is prepared by dissolving pre estimated amount of metal ferrite and an appropriate amount of citric acid in the deionized water by stirring for 30 minutes to obtain the clear solution. Solution (2) is prepared by dissolving specific pre estimated amounts of  $Ti(OC_4H_9)_4$  and citric acid in absolute ethyl alcohol by stirring for 30 minutes to get a clear solution. Solution (2) was very slowly added into solution(1) continuously by keeping the mixture continuously stirred for three hours. This gave the clear Solution (3). Then ammonia was added drop by drop to Solution (3), until the pH value was adjusted to 7.0. The system [11] should be acidic to maintain a clear solution as well as to prevent unwanted precipitation of either one or both the reactants before the gel formation and before combustion actually starts. The pH was determined using a precise pH meter. The pH is an important parameter that governs the characteristics of the Nano material. It is reported that as the pH of the solution increases the particle size also increases [14, 15]. Also as the pH increases, the weight losses are found to be small according to the literature. The obtained solution was evaporated with continuous stirring to form viscous sol precursors at  $80^{\circ}C$  & then dried at  $120^{\circ}C$ , for 24 to 48hrs. Then the viscous sol was heat treated for 3 hrs, at  $950^{\circ}C$ . Same procedure is repeated by varying the 'x' value ( $x=0.36$ ) at  $950^{\circ}C$ . So obtained BFTO powder samples were analysed by various characterization techniques.

### Characterisation of the Synthesised Samples

The phase identification and grain distribution of the sintered samples were identified using XRD X-ray Diffractometer (XRD) (Philips: PW1830), at University of Hyderabad, A.P. India and Scanning Electron Microscope (SEM) (SEM Hitachi- S520), at O.U., Hyderabad, A.P., INDIA. The FTIR (Schimadzu Perkin-Elmer 1310), at SAIF, IITM, India, was used to ascertain the metal-oxygen and metal-metal bond in the prepared ferrite sample.

## II. Results and Discussion

**XRD:** In the utilised X-ray powder diffraction (XRD) method, Cu K-alpha radiation (wavelength  $1.54178 \text{ \AA}$ ), is used for the scattering experiments. Figure 1 and 2 shows the XRD patterns of the  $BaFe_{(12-x)}Ti_xO_{19}$  (for  $x = 0.32$ ,  $x = 0.35^*$  and  $x = 0.36$ ) powders sintered at  $950^{\circ}C$  for 3 h. Both samples show single phase tetragonal structure, indicating the doping element has been successfully substituted into the structure. The average crystalline size was found to be in between 15 to 50 nm and was calculated using equation (1).

The Average grain size has been calculated using Debye – Scherrer's [16] equation (1) as shown below

$$D = [0.9\lambda / \beta_{1/2} \cos\theta] \text{ -----(1)}$$

Where

$\lambda$  = wave length of the x- ray beam

$\beta_{1/2}$  = Angular width at the half max intensity

$\theta$  = Braggs angle

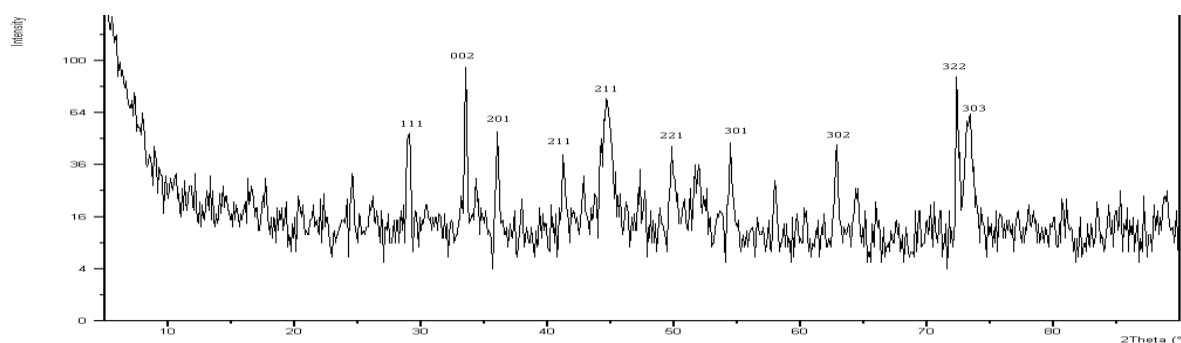


Figure 1: XRD graphs of Ti-doped barium ferrite ( $x=0.32$ ) at  $950^{\circ}C$  temperatures

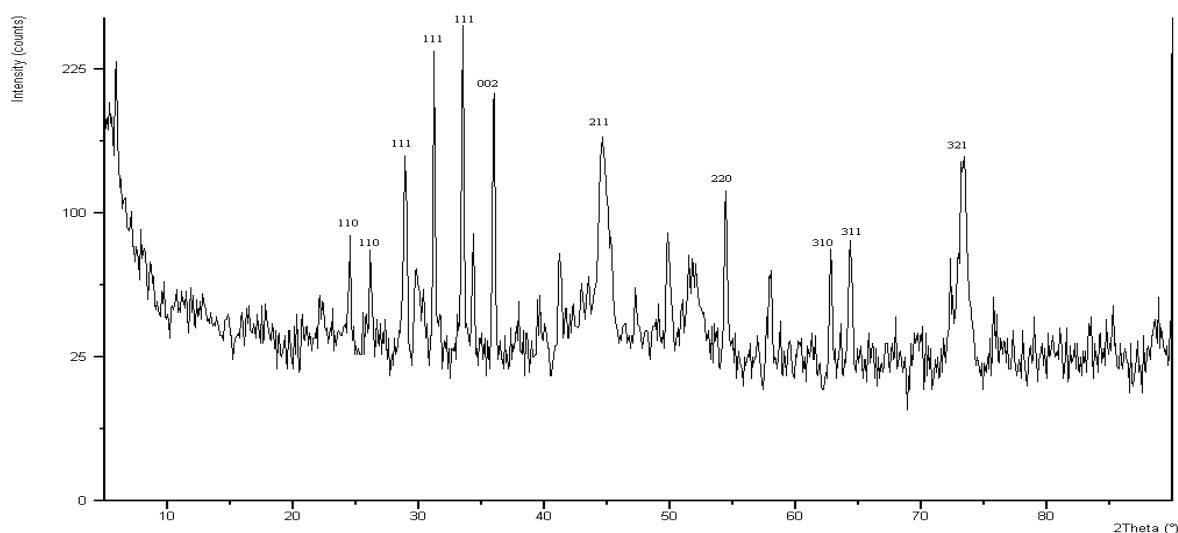


Figure 2: XRD graphs of Ti-doped barim ferrite ( $x=0.35^*$ ) at  $950^{\circ}C$  temperatures

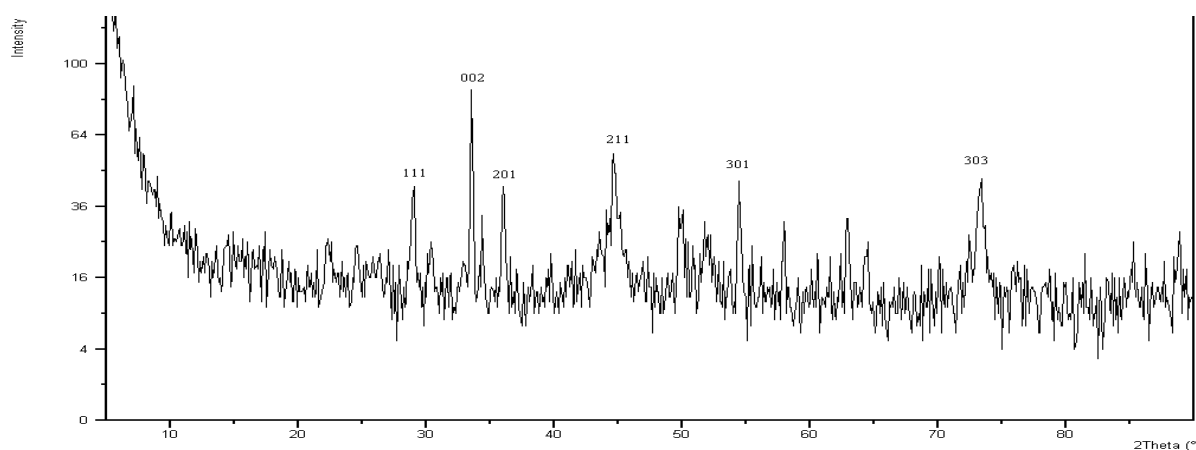


Figure 3: XRD graphs of Ti-doped barim ferrite ( $x=0.36$ ) at  $950^{\circ}C$  temperatures

Table1

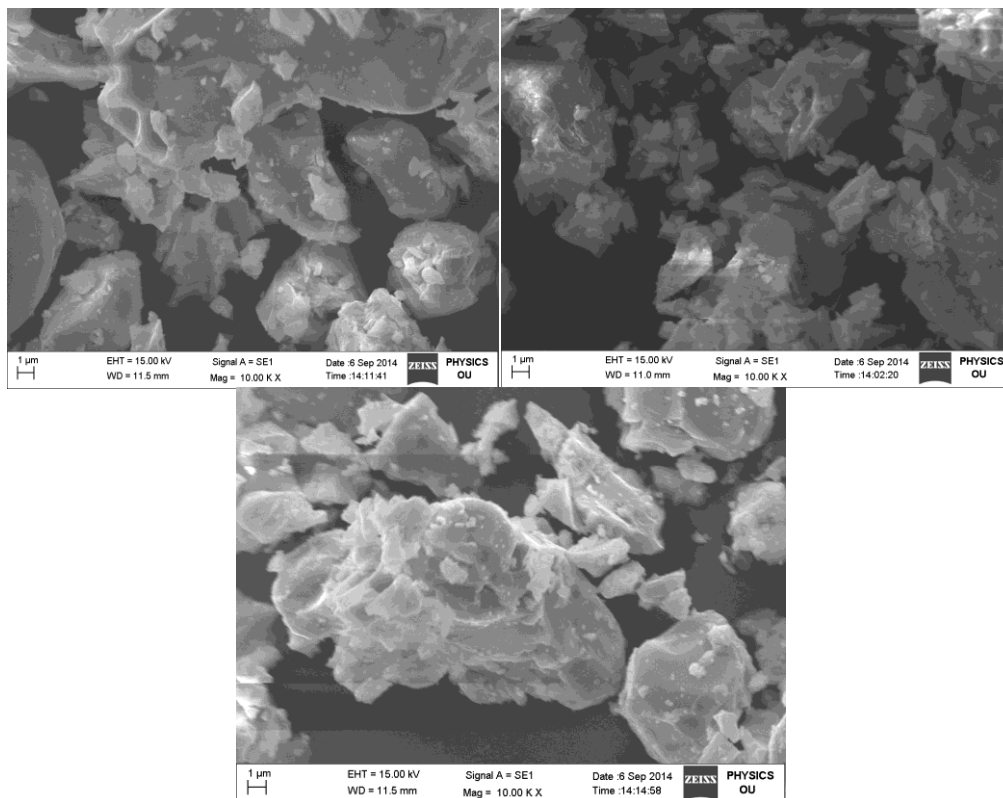
x=0.32		x=0.35*		x=0.36	
2θ(deg)	D(nm)	2θ(deg)	D(nm)	2θ(deg)	D(nm)
33.550	20.735	33.55	39.04	33.55	27.6471
36.0500	20.893	36.05	32.68	36.05	20.877
54.450	29.768	54.45	28.75	54.45	22.326

Table1: Average grain size D and 2θ values for x = 0.32, 0.35 and 0.36 at  $950^{\circ}C$  temperatures. (\* indicates this data has been taken from earlier communication by the same author[17])

Analysing the effect of varying the ‘x’ value, we can observe from figure(1,2 and 3) that for the sample ( $x=0.35^*$ ) sintered at  $950^{\circ}C$  shows well developed narrow peaks than the sample ( $x=0.32$  and  $0.36$ ) sintered at  $950^{\circ}C$ , which indicates that formation of nanostate is very nearly complete at  $x=0.35$  value.

**SEM:**

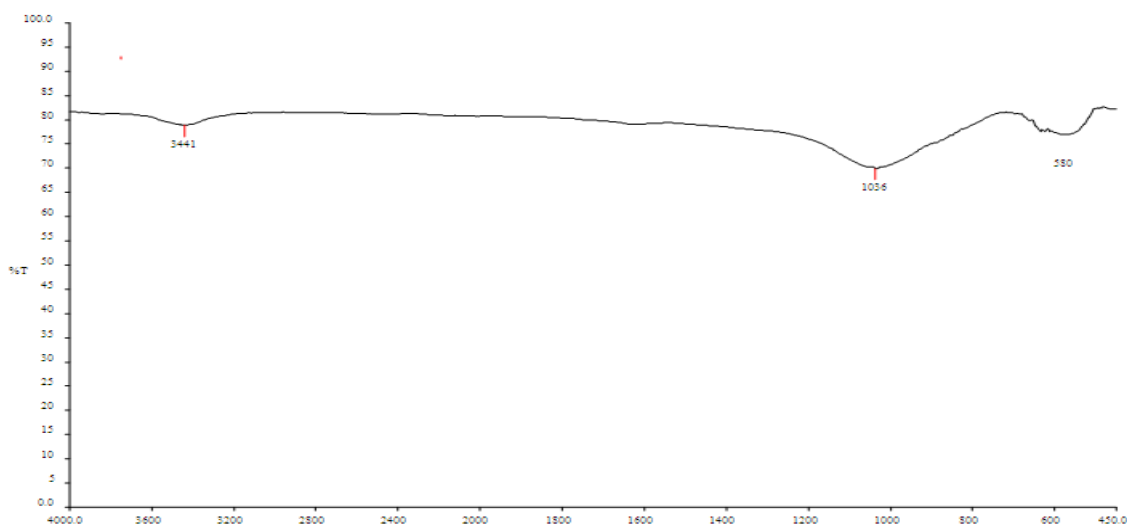
The SEM technique is used to characterize the morphology and size distribution of nanoparticles. The obtained SEM images of the synthesised barium ferrite samples are shown, in Figure-3. It is to be noticed that the particles of all samples exhibit plate – like nearly tetragonal shape. The particles are irregular in shape with compact arrangement and lies in the range of 10nm-40nm(using standard method of calculation). In some particles flakes of agglomerates are also observed. The samples obtained at different ‘x’ value at same tempering conditions show varying quality of crystallization.



**Figure 3: SEM pictures of Ti-doped barium ferrite at 'x'=0.32 , 'x'0.35\* and 'x' = 0.36 value at 950<sup>0</sup>C temperature**

**FTIR:**

Fourier Transform Infra-Red (FTIR) spectra have been recorded using Shimadzu Perkin-Elmer 1310 FTIR spectrophotometer with KBr pellets in the range 4000 – 400  $cm^{-1}$ . The FTIR of the BFTO powder (figure 4 ( $x=0.35^*$ )) shows characteristic peaks in the required region, i.e., 3418.34, 1618.51, 1400.80, 1080 and 543  $cm^{-1}$ . It is observed that a inverted peaks corresponding to 1618.51, 1400.80 and 3441  $cm^{-1}$  does not appear at the phase formation where the 'x' value of the BFTO powder ('x'=0.32 and 0.36) in the FTIR spectrum. This is attributed to the absence of the  $-CH_3$  group and C-H band at 'x'=0.32 and 0.36 possibly due to the varied 'x' value during doping of Titanium ion to Barium Ferrite is responsible for this. When the width of the FTIR inverted peaks are more, more of radiation is reflected. This reveals that in a given cross section more nanoparticles scattered radiation. Therefore the number of nanoparticles in that cross section are more. Hence the size of the nanoparticle less. Hence the broader peaks represent the formation of particles of smaller size.



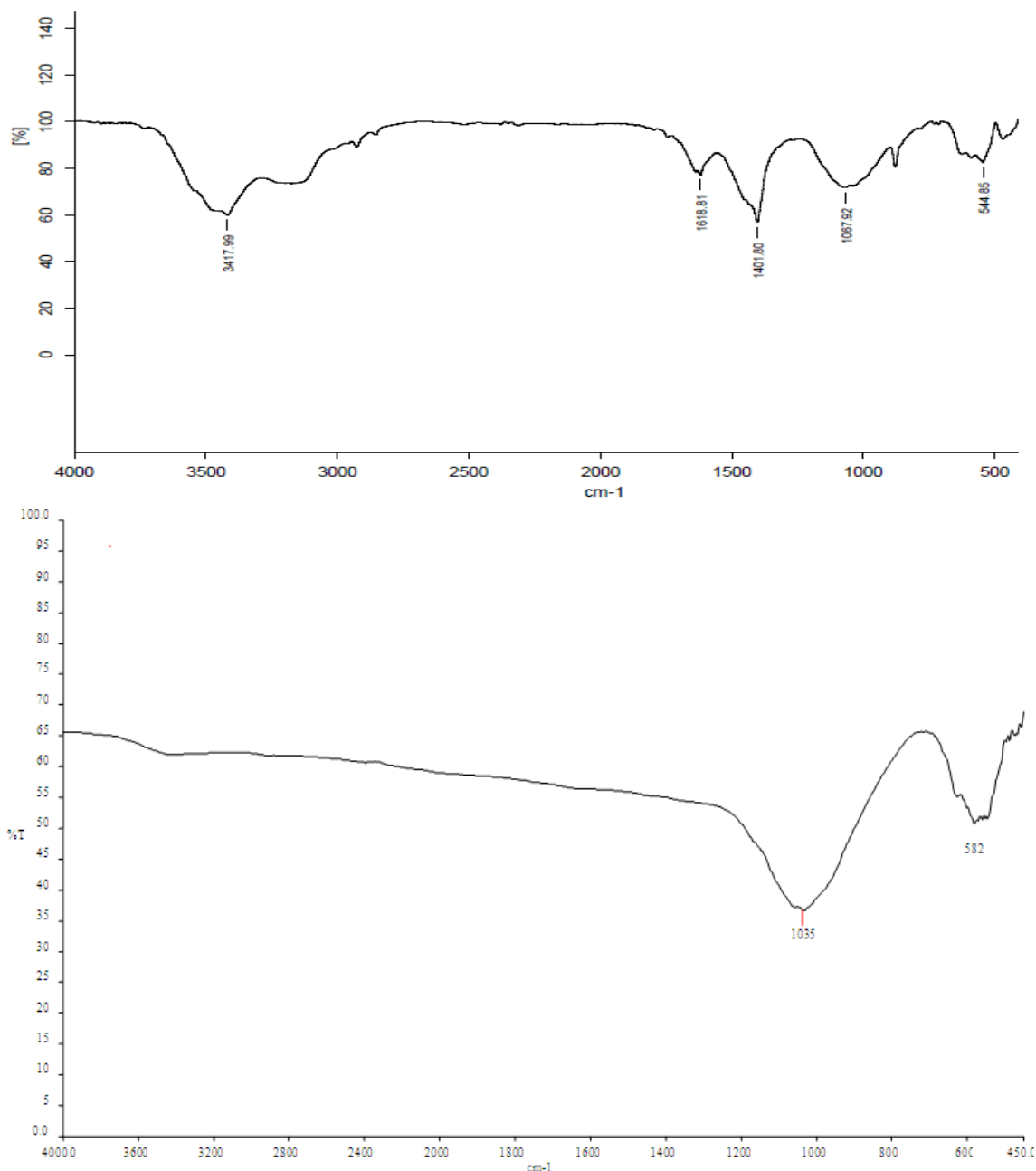


Figure 4: FTIR graphs of Ti-doped barium ferrite at 'x'=0.32 and 0.36 value at 950<sup>o</sup>C temperatures

Stretching Peak at 541 $cm^{-1}$  indicates existence of the metal-oxygen vibrational modes of the spinel compound, Stretching peak at 1080 $cm^{-1}$  indicates C-O, bending peak at 1400  $cm^{-1}$  indicates  $-CH_3$  [63], stretching peak at 1618  $cm^{-1}$  indicates remnants of C-H band and stretching peak at 3418  $cm^{-1}$  indicates O-H[1].

### III. Conclusion

In summary, we have successfully synthesized Ti- doped barium ferrite ( $x=0.32$  and  $x=0.36$ ) nanopowder by using Sol-gel technique. The formation of Titanium doped Nano ferrites has been con-firmed by XRD,SEM studies. FTIR studies on the same are also reported. The crystallite size is found to be in the range 15-40 nm.

### Acknowledgement

Authors are thankful to the DST and the SAIF, IIT Madras for helping in FTIR analysis. Authors wish to acknowledge Dr. Moneesha Fernandes , Scientist, department of Organic chemistry, National Chemical Laboratory, Pune ,India for her constant help and encouragement.

## References

- [1]. Wangchang Li , Xiaojing Qiao , Mingyu Li, Ting Liu and Peng H X. La and Co substituted M-type barium ferrites processed by sol-gel combustion synthesis. *Materials Research Bulletin* 2013; 48: 4449–4453.
- [2]. M.M. Costa, G.F.M. Pires Junior, A.S.B. Sombra, “Dielectric and impedance properties’ Studies of the lead doped (PbO)-Co<sub>2</sub>Y type hexaferrite (Ba<sub>2</sub>Co<sub>2</sub>Fe<sub>12</sub>O<sub>22</sub> (Co<sub>2</sub>Y)),” *International Journal of Materials Chemistry and Physics*, 123, pp 35–39, 2010.
- [3]. Chen Q, Du PY, Huang WY, Jin L, Weng WJ and Han GR. Ferrite with extraordinary electric and dielectric properties prepared from self-combustion technique. *Appl Phys Lett* 2007; 90: 132907.
- [4]. Sun GB, Dong BX, Cao MH, Wei BQ and Hu CW . Hierarchical Dendrite-Like Magnetic Materials of Fe<sub>3</sub>O<sub>4</sub>, γ-Fe<sub>2</sub>O<sub>3</sub> and Fe with High Performance of Microwave Absorption. *Chem Mater* 2011; 23: 1587–93.
- [5]. Ohkoshi S, Kuroki S, Sakurai S, Matsumoto K, Sato K and Sasaki S. A millimeter-wave absorber based on gallium-substituted epsilon-iron oxide nanomagnets. *Angew Chem Int Ed Engl* 2007; 46: 8392–8395.
- [6]. Zheng H, Dong YL, Wang X, Weng WJ, Han GR, Ma N and Du PY. Super High Threshold Percolative Ferroelectric/Ferrimagnetic Composite Ceramics with Outstanding Permittivity and Initial Permeability. *Angew Chem Int Ed Engl* 2009; 48: 8927–8930.
- [7]. S. Maensiri, C. Masingboon, B. Boonchom and S. Seraphin, “A Simple Route to Synthesize Nickel Ferrite (NiFe<sub>2</sub>O<sub>4</sub>) Nanoparticles Using Egg White,” *Scripta Materialia*, Vol. 56, No. 9, 2007, pp. 797-800. doi:10.1016/j.scriptamat.2006.09.033
- [8]. Ruan SP, Xu BK, Suo H, Wu FQ and Xiang SQ. Microwave absorptive behavior of ZnCo-substituted W-type Ba hexaferrite nanocrystalline composite material. *J Magn Magn Mater* 2000; 212: 175–177.
- [9]. Bernd Halbedel , Dagmar Hülsenberg, Stefan Belau, Uwe Schadewald and Michael Jakob . Synthese und Anwendungen von maßgeschneiderten BaFe<sub>12-2x</sub>Al<sub>x</sub>Bi<sub>x</sub>O<sub>19</sub>-Pulvern. *cfi/Ber DKG* 2005; 82:182–188.10.
- [10]. Rohde & Schwarz. A new dimension in compactness. *News* 199/09. 2009, p. 70–72.
- [11]. Swadesh K Pratihari, Mayank Garg, Supreet Mehra and S. Bhattacharyya. Phase Evolution and Sintering Kinetics of Hydroxyapatite Synthesized by Solution Combustion Technique. *J Mater Sci Mater Med*. 2006 Jun;17(6):501-7
- [12]. Alamolhoda S , Seyyed Ebrahimi SA and Badiei A. Optimization of the Fe/Sr Ratio in Processing of Ultra-Fine Strontium Hexaferrite Powders by a Sol-Gel Auto-combustion Method in the Presence of Trimethylamine. *Iranian Int J Sci* 2004; 5(2):173-179.
- [13]. (a)Molaei MJ, Ataie A, Raygan S, Rahimpour MR, Picken SJ, Tichelaar FD,
- [14]. Legarra E and Plazaola F. Magnetic property enhancement and characterization of nano-structured barium ferrite by mechano-thermal treatment. *Materials characterization* 2012; 63: 83 – 89.
- [15]. 13.(b)Molaei MJ , Ataie A, aygan S, Picken SJ and Tichelaar FD. Investigation on the Effects of
- [16]. Milling Atmosphere on Synthesis of Barium Ferrite/Magnetite Nanocomposite. *J Supercond*
- [17]. *Nov Magn* 2012; 25: 519–524.
- [18]. Praveena K, Sadhana K, Srinath S and Murthy SR. Effect of pH on structural and magnetic properties of nanocrystalline Y<sub>3</sub>Fe<sub>5</sub>O<sub>12</sub> by aqueous co-precipitation method. *Material Research Innovations* 2013;18:69-75.
- [19]. Kim T , Nasu S and Shima M. Growth and magnetic behavior of bismuth substituted yttrium iron garnetnanoparticles. *Journal of Nanoparticle Research* 2007; 9(5): 737-743.
- [20]. Radek Zboril, Miroslav Mashlan and Dimitris Petridis. Iron(III) Oxides from Thermal
- [21]. Processess, Synthesis,Structural and Magnetic Properties, Mossbauer Spectroscopy Characterization, and Applications. *Chemistry of Materials* 2002;14: 969-982.
- [22]. Aparna AR et.al. Synthesis and Structural, Morphological and FTIR Studies on Ferrite
- [23]. Powders BaFe<sub>(12-x)</sub>Ti<sub>x</sub>O<sub>19</sub>, Using Sol-Gel Method. Part N: *Journal of Nanoengineering and Nanosystems* 2015;Id: JNN-14-0052.R1(In Press).